

## The CMS commissioning

P. MERIDIANI

*Eidgenössische Technische Hochschule Zürich - Zürich, Switzerland*

(ricevuto l'8 Ottobre 2010; pubblicato online il 2 Febbraio 2011)

**Summary.** — After nearly two decades of design, construction and commissioning, the CMS detector was operated with colliding LHC proton beams for the first time in November and December 2009. Collision data was recorded at centre-of-mass energies of 0.9 and 2.36 TeV, and analyzed with a fast turn-around time by the CMS Collaboration. In this talk I will review the commissioning condition at the start of the proton collision operation and a selection of commissioning results from the collision analysis. The proposed results show an excellent performance of the CMS detector and a very good agreement with the expectations from simulation for a hadron collider detector at start-up. The results are thus very encouraging for the start of the 7 TeV physics run.

PACS 29.40.Vj – Calorimeters.

PACS 29.40.Wk – Solid-state detectors.

### 1. – Introduction

The CMS experiment [1] recorded the first LHC proton-proton collisions on Monday the 23rd of November, 2009. In the weeks that followed, CMS collected approximately 390 thousand collision events at a centre-of-mass energy  $\sqrt{s} = 0.9$  TeV and 20 thousand events at  $\sqrt{s} = 2.36$  TeV with good detector conditions and the magnet switched on at the nominal value of 3.8 T. This corresponds to about  $12 \mu\text{b}^{-1}$  of integrated luminosity. The recorded data sample was used to start assessing the general quality and the proper functioning of the detector, and to evaluate the performance of the algorithms and the modeling of the detector response in the simulation. This is a crucial step in preparation for physics analyses.

### 2. – The CMS detector in a nutshell

A detailed description of the CMS detector can be found elsewhere [1]. The central feature of the CMS apparatus is a superconducting solenoid of 6 m internal diameter, providing a uniform magnetic field of 3.8 T. Within the magnetic field are the tracker, the electromagnetic calorimeter (ECAL) and the hadron calorimeter (HCAL). Gas-based

detectors embedded in the steel return yoke are used to measure and identify muons. The tracker is made of 1440 silicon-pixel and 15148 silicon-strip detector modules and measures charged particles trajectories within the pseudorapidity range  $|\eta| < 2.5$ . ECAL is a homogeneous calorimeter made of 75848 lead tungstate scintillating crystals. It consists of a central barrel covering the pseudorapidity region up to  $|\eta| = 1.5$ ; the coverage for precision measurements extends up to  $|\eta| = 2.6$  including two endcaps. A silicon preshower detector also covers the region between  $|\eta| = 1.6$  and  $|\eta| = 2.6$ . HCAL is made of 70000 brass/scintillator plates. An additional hadron detector is located outside the barrel region occupied by HCAL, and provides additional information to reject residual hadronic showers. These calorimeters cover an acceptance of  $|\eta| < 3$ . The acceptance region of  $3 < |\eta| < 5$  is covered by a quartz very forward calorimeter.

### 3. – CMS status at start-up

In the years preceding the first LHC proton-proton collisions, CMS recorded and analysed more than a billion events with muons from various sources. Three cosmic ray runs in 2006 (done on surface before CMS was integrated in the pit), 2008 and 2009 recorded about 300 million cosmic ray muon events each. Over a million beam halo muons were recorded during LHC commissioning in 2008 and 2009, as well as more than a thousand so-called beam-splash events. In particular, these beam-splash events occur when LHC dumps a single bunch of the beam on a collimator about 150 m upstream from CMS, leading to a flood of muons traveling through the detector simultaneously. This sample of data is particularly useful to check the synchronization of the detectors, especially for the calorimeter cells. Using this data it was possible to set the ECAL channel-to-channel synchronization to better than 1 ns [2], and within 2 ns for the HCAL [3]. Detailed analysis of these events resulted also in crucial improvements in the alignment of the detector, modeling of the magnetic field, understanding of the response of different subdetectors to muons, calibration and noise characteristics. The results of these studies are described in 23 performance papers [4]. For example the relative momentum resolution for muons crossing the barrel part of the detector was measured to be better than 1% at 10 GeV/c and about 8% at 500 GeV/c, the latter being only a factor of two worse than expected with ideal alignment conditions [5]. In addition, the positions of the silicon tracker modules were determined to a precision of 3–4  $\mu\text{m}$  RMS in the barrel and 3–14  $\mu\text{m}$  RMS in the endcap in the most sensitive coordinate. The track parameter resolutions obtained with this alignment were shown to be at the start-up already close to the design performance [6]. An important outcome of the cosmic runs was also the measurement of the magnetic field in the steel of the barrel yoke to a precision from 3 to 8%, which allowed to significantly improve the finite-element model of the magnetic field in the return yoke. In fact, the model was initially found to overestimate the field by about 20% due to the tightness of the physical boundaries imposed in the calculation [7]. The overall health of the CMS detector was indeed very good at the start-up, in fact more than 99% of the overall channels were operational.

### 4. – CMS commissioning with beam

4.1. *Tracking.* – The CMS silicon tracker and tracking algorithms performed very well from the start of data taking. Beam spot and primary vertices were reconstructed with high efficiency and resolution close to the expectation from simulation [8].

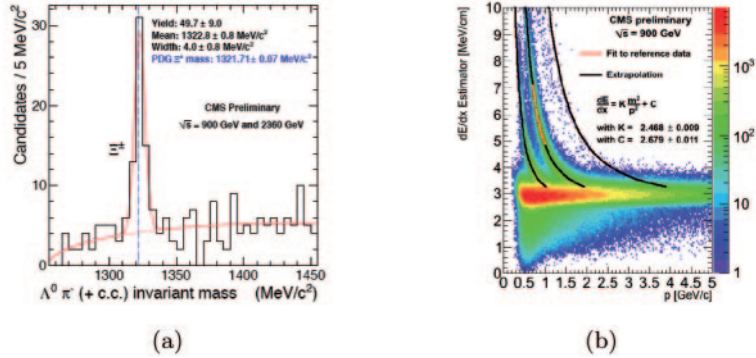


Fig. 1. – (Colour on-line) (a)  $\Lambda^0 \pi^-$  invariant mass plot with a fit for the  $\Xi^-$  and (b)  $dE/dx$  vs.  $p$  in data collected at 0.9 TeV (the red line gives a fit with proton mass assumption, in a restricted  $p$  range, while black lines show extrapolations).

The performance of the tracker was demonstrated with the help of long-lived resonances, decaying to charged hadrons off the primary interaction vertex [8]. Within hours after the first run, the invariant mass peaks of the decays of the neutral kaon  $K_S \rightarrow \pi^+ \pi^-$  and of the  $\Lambda^0 \rightarrow p \pi^-$  (and their charge conjugates) were reconstructed, with a mass scale correct to better than 0.1% and good agreement between data and simulation for the resolution [8]. The resonances identified this way can also be combined with other charged hadrons to reconstruct resonances such as the  $K^*(892)$  and the  $\Xi^- (\Xi^+)$  (fig. 1(a)). Also in this case the mass peaks show an agreement within statistical precision with the literature numbers [8].

Exploiting the silicon tracker capabilities for particle identification at low momentum, since the energy deposited in the silicon layers allows to measure the energy loss rate of the charged particle (fig. 1(b)) was also possible to enhance kaons in extraction of the  $\Phi(1020)$  meson signal.

As a commissioning of the tracker capability to tag bottom jets, the measured distribution of some relevant  $b$ -tagging related variables were compared with the expected light, charm and bottom jet contributions from simulation [8]. All the basic  $b$ -tagging variables were found to be well described by simulation.

**4.2. Calorimeters.** – The electromagnetic calorimeter barrel was intercalibrated at start-up to better than 1.5% using cosmics and test beam electrons [9]. The invariant-mass distributions of photon pairs detected in the ECAL barrel from the  $\pi^0$  and  $\eta$  decay were used as the first performance and commissioning tool, and will be used later with more statistics for calibration purposes. These distributions, shown in fig. 2 for  $\pi^0$  both in data and simulation, do not contain yet corrections for shower containment, thresholds and energy loss. The peak resolution and the ratio of signal to background are in good agreement between data and simulation. The energy scale is also seen to agree within 2% with the expectation from simulation.

**4.3. “Particle Flow”, jets and missing energy.** – CMS design is particularly appropriate for the “Particle Flow” approach due to the combination of a strong magnetic field, precise silicon tracker and an electromagnetic calorimeter with fine lateral segmentation. The goal of this method is to reconstruct all the stable particles in the event (electrons, muons, photons and charged and neutral hadron components) combining the information

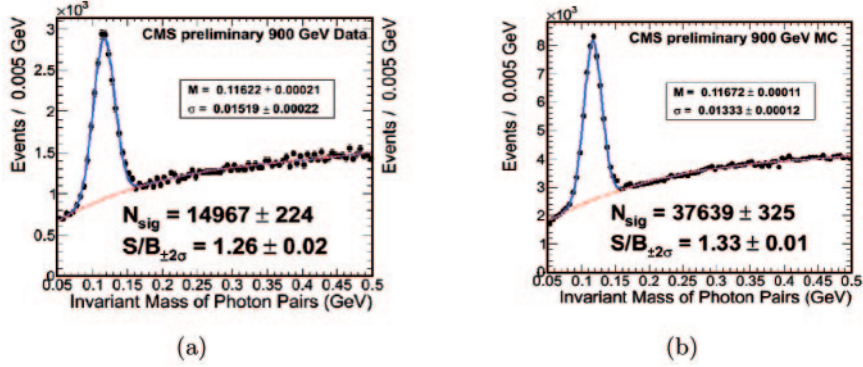


Fig. 2. – Uncorrected photon-pair invariant-mass distributions in data (a) and simulation (b) in the region around the  $\pi^0$  resonance.

from all CMS subdetectors. Simulation studies have shown that this could lead to an improvement of about a factor two in the resolution for jets at low  $p_T$  ( $< 50$  GeV) and for missing transverse energy. Key ingredients of this approach have been commissioned with the 0.9 TeV collision dataset. The angular matching between tracks and calorimeter deposits was shown to be reproduced very well by the simulation [10]. In addition also the single particle response in the calorimeters, measured as the average response of a track with the associated electromagnetic (ECAL) and hadronic calorimeter (HCAL) clusters, was checked to be well reproduced by the simulation without additional tuning, as it is shown in fig. 3(a). These aspects constitute a first important step in the commissioning of the “Particle Flow” algorithm. In CMS jets are reconstructed combining different information: using calorimeter energy deposits only; using calorimeter energy deposits with track corrections; using particle-flow candidates. The measured and the corresponding simulated jet  $p_T$  spectra as reconstructed using particle-flow information are shown in fig. 3(b) for an inclusive jet selection. More details can be found here [11].

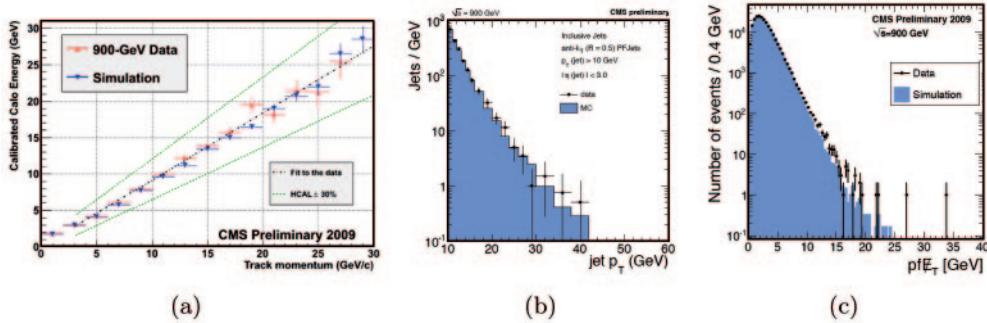


Fig. 3. – (Colour on-line) (a) Average calorimeter response as a function of the track momentum for the 900 GeV data (red upwards triangles) and simulation (blue downwards triangles). The dash-dotted line is a linear fit to the data, and the dashed lines show the same fit with a HCAL raw response changed by  $\pm 30\%$ . Comparison of data and simulation of the inclusive jet  $p_T$  spectrum (b) and of the missing  $E_T$  distribution (c) in minimum bias events at  $\sqrt{s} = 0.9$  TeV. Both are reconstructed using “Particle-Flow” information.

Careful studies of anomalous energy deposits were performed identifying cleaning procedures for the different noise sources [12]. The missing transverse-energy distribution after the cleaning procedure, as measured in minimum bias data, has been compared with the simulation showing a good agreement in the resolution and in the tails (fig. 3(c)).

## 5. – Conclusions

The CMS Collaboration has extracted several performance results from the first  $12\mu\text{b}^{-1}$  of collision data delivered by the LHC, progressing on the understanding of the detector performance after the initial commissioning with cosmic-ray data and the first dumps of the LHC beam. The quality of the agreement with the detector simulation is outstanding for a collider experiment at start-up. It should be noted, however, that the data collected so far correspond to less than a millisecond of data taking at the nominal LHC luminosity. Further commissioning of the trigger system, lepton and jet reconstruction and selections will be performed with the data from the physics run at a center-of-mass energy  $\sqrt{s} = 7\text{TeV}$ .

\* \* \*

We wish to congratulate our colleagues in the CERN accelerator departments for the excellent performance of the LHC machine. We thank the technical and administrative staff at CERN and other CMS institutes, and acknowledge support from: FMSR (Austria); FNRS and FWO (Belgium); CNPq, CAPES, FAPERJ and FAPESP (Brazil); MES (Bulgaria); CERN; CAS, MoST and NSFC (China); COLCIENCIAS (Colombia); MSES (Croatia); RPF (Cyprus); Academy of Sciences and NICPB (Estonia); Academy of Finland, ME and HIP (Finland); CEA and CNRS/IN2P3 (France); BMBF, DFG and HGF (Germany); GSRT (Greece); OTKA and NKTH (Hungary); DAE and DST (India); IPM (Iran); SFI (Ireland); INFN (Italy); NRF and WCU (Korea); LAS (Lithuania); CINVESTAV, CONACYT, SEP and UASLP-FAI (Mexico); PAEC (Pakistan); SCSR (Poland); FCT (Portugal); JINR (Armenia, Belarus, Georgia, Ukraine, Uzbekistan); MST and MAE (Russia); MSTDS (Serbia); MICINN and CPAN (Spain); Swiss Funding Agencies (Switzerland); NSC (Taipei); TUBITAK and TAEK (Turkey); STFC (United Kingdom); DOE and NSF (USA).

## REFERENCES

- [1] THE CMS COLLABORATION, *JINST*, **3** (2008) S08004.
- [2] THE CMS COLLABORATION, *JINST*, **5** (2010) T03011.
- [3] THE CMS COLLABORATION, *JINST*, **5** (2010) T03013.
- [4] THE CMS COLLABORATION, *JINST*, **5** (2010) T03001-T03020 and P03007.
- [5] THE CMS COLLABORATION, *JINST*, **5** (2010) T03022.
- [6] THE CMS COLLABORATION, *JINST*, **5** (2010) T03009.
- [7] THE CMS COLLABORATION, *JINST*, **5** (2010) T03021.
- [8] THE CMS COLLABORATION, *CMS Physics Analysis Summary*, TRK-10-001 (2010).
- [9] THE CMS ECAL GROUP, *JINST*, **3** (2008) P10007.
- [10] THE CMS COLLABORATION, *CMS Physics Analysis Summary*, PFT-10-001 (2010).
- [11] THE CMS COLLABORATION, *CMS Physics Analysis Summary*, JME-10-001 (2010).
- [12] THE CMS COLLABORATION, *CMS Physics Analysis Summary*, JME-10-002 (2010).